Atmos. Meas. Tech. Discuss., 5, 6323–6355, 2012
www.atmos-meas-tech-discuss.net/5/6323/2012/
doi:10.5194/amtd-5-6323-2012

Atmospheric Measurement Techniques Discussions

Quantification of uncertainties of water vapour column retrievals using future instruments

H. Diedrich, R. Preusker, R. Lindstrot, and J. Fischer

Institut für Weltraumwissenschaften, Freie Universität Berlin,
Carl-Heinrich-Becker-Weg 6–10, 12165 Berlin, Germany

Received: 12 July 2012 – Accepted: 28 August 2012 – Published: 6 September 2012

Correspondence to: H. Diedrich (hannes.diedrich@wew.fu-berlin.de)

Published by Copernicus Publications on behalf of the European Geosciences Union.

Abstract

This study presents a quantification of uncertainties of water vapour retrievals based on near infrared measurements of upcoming instruments. The concepts of three scheduled spectrometer were taken into account: OLCI (Ocean and Land Color Instrument) on Sentinel-3, METimage on MetOp (Meteorological Operational Satellite) and FCI (Flexible Combined Imager) on MTG (Meteosat Third Generation). Optimal estimation theory was used to estimate the error of an hypothetical total water vapour column retrieval for 27 different atmospheric cases. The errors range from 100 % in very dry cases to 2 % in humid cases with a very high surface albedo. Generally the absolute uncertainties increase with higher water vapour column content due to H_2O-saturation and decrease with a brighter surface albedo. Uncertainties increase with higher aerosol optical thickness, apart from very dark cases. Overall the METimage channel setting enables the most accurate retrievals. The retrieval using the MTG-FCI buildup has the highest uncertainties apart from very bright cases.

A retrieval using two absorption channels increases the accuracy, in some cases by one order of magnitude, in comparison to a retrieval using just one absorption channel. On the other hand, a retrieval using three absorption channels has no significant advantage over a two-absorption channel retrieval.

Furthermore, the optimal position of the absorption channels was determined using the concept of the "information content". For a single channel retrieval a channel at 900 or 915 nm has the highest mean information contents over all cases. The second absorption channel is ideally weakly correlated with the first one, thus positioned at 935 nm, in a region with stronger water vapour absorption.

1 Introduction

Water vapour is the most important greenhouse gas in the earth's atmosphere and has a strong connection to various feedback mechanisms on climate (Solomon, 2007).

AMTD
5, 6323–6355, 2012

Detecting local and global trends in the water vapour field is therefore an important task for climate research. Satellite remote sensing can provide high spatial and temporal resolutions. Water vapour detection over ocean surfaces has been done since the 1980s with microwave radiometers (Schluessel and Emery, 1990). However, the detection of the water vapour column over land surfaces is much more complicated. Emissivities of land surfaces are highly heterogeneous and mostly unknown in the microwave spectrum. Consequently reflected sunlight in the near-infrared (NIR) is measured and analysed. This fact limits the detection of water vapour to cloud free areas.

There are already some instruments and retrievals which operationally retrieve water vapour over cloud free land surfaces, for example MERIS (MEdium Resolution Imaging Spectrometer) on ENVISAT (Lindstrot et al., 2012; Fischer, 2010) The existing retrievals are various but use a basic principle, the differential absorption technique (Albert et al., 2001, 2005; Gao et al., 1993; Bartsch et al., 1996). The comparison of radiances in a window channel with radiances in an absorption channel provides information about the total columnar water vapour (TCWV).

However, there are a number of error sources for the retrieval of water vapour from near infrared measurements: one part of the uncertainty is due to technical constraints, such as instrumental noise or spectral and absolute calibration of the spectrometers. On top of that, the retrieval is based on various assumptions with respect to, e.g. scattering in the atmosphere or the vertical temperature profile. One goal of this study is the quantification of uncertainties of an hypothetical water vapour retrieval using three future concepts of spectrometers. Additionally, we aim to find out how to improve the accuracy of such retrieval by determining the optimal channel setting for the water vapour remote sensing. Although there is no information about the measurement accuracies and the actual retrieval, one can estimate the uncertainties using the optimal estimation theory and the concept of information content.

AMTD
5, 6323–6355, 2012

2 Instruments

2.1 OLCI

The Ocean and Land Color Instrument (OLCI) is planned to be the follower of MERIS (Medium Resolution Imaging Spectrometer). It will be installed on the Sentinel-3 orbiter which is part of the GMES (Global Monitoring for Environment and Security) program. It is scheduled to be launched in 2013 at the earliest with a lifetime of approximately more than 12 years (fuel for five more years is going to be available). To provide a better temporal resolution it is planned to operate two identical platforms which orbit the earth on sun-synchronous tracks in about 815 km height with a local time of descending node (LTDN) at around 10:00 to 10:30 a.m. OLCI will be build up of five identical cameras in a fan shape alignment (role model: MERIS). It will measure the radiation reflected from the earth in the visible and near infrared spectrum. The spatial resolution of the spectrometer will be 300 m (full resolution) which can be downscaled to reduced resolution (1200 m). The spectrometer can sample a line of 1300 km (field of view: 68.5°) at once. The observation geometry will be tilted by 12° to reduce sun glint effects. With a two-satellite composition global coverage is achieved within 4 days. Every 27 days a cycle is repeated. OLCI will be upgraded in comparison to MERIS from 15 to 21 spectral channels in the wavelength range of 0.4 to 1.02 µm. The planned channels in the near-infrared, relevant for water vapour retrievals, are shown in Fig. 1 (http://www.ioccg.org/sensors/olci.html).

2.2 METimage

METimage will be a multispectral radiometer, mounted on the second generation of MetOp (Meteorological Operational Satellite) in the network which continues the EUMETSAT polar system (EPS). This framework consists of 3 polar orbiting MetOp satellites and its prime objective is to provide continuous, long term data sets of meteorological quantities. Metop-A was already launched in 2006. Metop-B and Metop-C will

AMTD
5, 6323–6355, 2012

follow. Center of the METimage concept is a rotating telescope developed by Jena-Optik. The visual/infrared imager (VII) will detect the sun light, reflected by the earth, in the visible and near infrared spectrum from 0.4 to 14 µm. A spatial resolution of maximum 250 m and a field of view of 110° (swath approximately 2800 km) is expected. The radiometer scans 20 pixel simultaneously with a field of view of 1° (20 km). The channel constellation and the number of channels has not been finally decided yet. A 20-channel or a 30-channel concept face a choice. The Institute for Space Science at the Free University Berlin was asked to find out the best channel position and combination for the water vapour remote sensing. The planned channels in the near-infrared, relevant for water vapour retrievals, are shown in Fig. 2 (http://www.eumetsat.int).

2.3 MTG-FCI

The Meteosat Third Generation (MTG) system is going to replace the Meteosat Second Generation (MSG). The concept of geostationary satellites is based on two three-axis-stabilized platforms, the MTG-I (imager) and the MTG-S (sounder), positioned at three orbiting positions. The scheduled launch is in 2017. A spectrometer will be installed on MTG-I, the flexible combined imager (FCI). It can detect the electromagnetic radiation in 16 channels rather than 12 on MSG between 0.4 and 13.3 µm with an expected spatial resolution of maximal 1 km between 0.4 and 2.1 µm and a spatial resolution of 2 km between 3.8 and 13.3 µm. The planned channels in the near-infrared, relevant for water vapour retrievals, are shown in Fig. 3 (http://www.eumetsat.int).

3 Theory

3.1 Radiative transfer calculations

In this study the radiative transfer model MOMO was used for the radiative transfer calculations in order to determine the sensitivities of certain channels to different atmospheric properties. It is based on the Matrix Operator Method (Plass et al., 1973;

AMTD
5, 6323–6355, 2012

Grant and Hunt, 1969a,b; Twomey et al., 1966). MOMO is a one-dimensional model with a coupled ocean-atmosphere-system. It derives the upward and downward radiative fluxes on the borders of the prior defined vertical layers for selectable zenith- and azimuth-angles (Fischer and Grassl, 1984; Hollstein and Fischer, 2012). For this investigation radiative transfer calculations have been performed for a part of the $\rho\sigma\tau$-band in the near infrared from 880 to 960 nm. The scattering properties of different atmospheric components like ice-clouds or aerosols were calculated using a Mie code based on Wiscombe (1980). The absorption coefficients of the atmospheric gases (mainly H_2O and O_2) were computed with the k-distribution-method (Bennartz and Fischer, 2000). Information about the location and width of the absorption lines originate from the HITRAN-database (Rothman et al., 2010).

3.2 Quantification of uncertainies using optimal estimation

3.2.1 Best-estimate-error

A measurement is never exact, there is always an uncertainty. The result of a measurement is thus composed of the measurement value itself (y) and the measurement uncertainty (σ_y). For tasks in the remote sensing the measurements are mostly TOA radiances. The determination of the measurement error of the instrument is realizable by calibration and comparison-measurements. Most techniques retrieve physical properties out of radiance-measurements using complicated inversions. Consequently, the retrieved quantities (combined in the state vector $\boldsymbol{x}$) will also be uncertain ($\boldsymbol{\sigma_x}$ is the error of the retrieved quantity). Commonly the inversions work with an iterative optimization of a forward model F which uses lots of additional (prior-)information (model parameters p) which are also contaminated with errors $\boldsymbol{\sigma}_p$:

$$\boldsymbol{y} \pm \boldsymbol{\sigma_y} = \boldsymbol{F}(\boldsymbol{x} \pm \boldsymbol{\sigma_x}, p \pm \boldsymbol{\sigma}_p). \quad (1)$$

For instance, the TOA radiance, reflected from the earth, depends on the surface albedo, the aerosol load, the water vapour content, clouds, temperature etc. These

AMTD
5, 6323–6355, 2012

parameters can only be measured with a certain accuracy. The pivotal question is thus: how can we determine the uncertainty of the retrieved atmospheric property σ_x without special knowledge of the retrieval technique? One method was introduced by Rodgers (2000). The procedure uses amongst others the Bayes' theorem and assumes Gauss-distributed errors. For the detailed derivation I refer to the book. In the following only an overview of the method is presented.

The influence of an individual parameter on the retrieved state can be calculated, provided that the senitivity of the measurement to the parameter is known. For example, in case the uncertainty of a model parameter is large, but the sensitivity of the measurement to the parameter is negligible, there is no significant increase in the uncertainty of the retrieved state. The influence of individual parameters on the measurement can be simulated with a radiative transfer model (e.g. MOMO). The Jacobian of the radiance according to a certain parameter can be approximated by the change in radiance in response to a small change in the parameter, while keeping all other parameters constant.

Dependent on the number of channels and parameters, that are accounted for in the error propagation, a matrix $\mathbf{K}^p$ is spanned, containing information about the sensitivity of the parameters to the measurement. Practically, these are the derivatives of the radiance in a channel i to the variation of the jth model-parameter:

$$\mathbf{K}^p_{i,j} = \left\{ \frac{\delta y_i}{\delta p_j} \right\}. \tag{2}$$

Here, local linearity must be assumed. The uncertainty of the prior knowledge of each model parameter of determination of the parameters are stored in a covariance matrix $\mathbf{S}^p$:

$$\mathbf{S}^p_{i,j} = \left\{ c_{i,j} \sigma_{p,i} \sigma_{p,j} \right\}, \tag{3}$$

where $\sigma_{p,i}$ is the uncertainty in unity of standard deviation of the ith model-parameter and $c_{i,j}$ the linear correlation coefficient between the ith and jth parameter. For many

AMTD
5, 6323–6355, 2012

applications the correlation is zero, resulting in diagonal matrices $\mathbf{S}^p$ are occupied. The measurement error covariance matrix $\mathbf{S}^y$ is defined as:

$$\mathbf{S}^y_{i,j} = \left\{ c_{i,j} \sigma_{y,i} \sigma_{y,j} \right\}, \tag{4}$$

where $\sigma_{y,i}$ is the measurement error in unity of standard deviation for the ith channel of the spectrometer and $c_{i,j}$ the correlation between the error which is zero for standard spectrometer, so $\mathbf{S}^y$ the diagonal elements:

$$(\sigma^y_{i,i})^2 = (L_i/\mathrm{SNR}_i)^2 + \Delta_i^2, \tag{5}$$

where L_i is the measured radiance in channel i, SNR_i the signal to noise ratio (SNR = y/σ_y) and Δ_i the uncertainty of the absolute calibration of the channel i. The matrix $\mathbf{K}$ carries information about the sensitivities of the measurement in the ith channel to the jth element of the state vector $\boldsymbol{x}$, so the derivatives of radiance to the retrieval-quantity:

$$\mathbf{K}_{i,j} = \left\{ \frac{\delta y_i}{\delta x_j} \right\}. \tag{6}$$

Finally the error covariance matrix of the state vector is defined by:

$$\mathbf{S}^x = \left\{ c_{i,j} \sigma_{x,i} \sigma_{x,j} \right\}. \tag{7}$$

It describes the uncertainties of the retrieved quantity. The square route of the diagonal elements of $\mathbf{S}^x$ specifies the error in the unit of the retrieved value and is thus the sought after quantity.

According to Rodgers (2000) the approach to calculate $\boldsymbol{S}^x$ is as follows: first, the model-uncertainty $\mathbf{S}^e$ is derived by propagating the model-parameter-uncertainty $\mathbf{S}^p$ into the measurement space and adding the measurement uncertainty $\mathbf{S}^y$:

$$\mathbf{S}^e = \mathbf{S}^y + \mathbf{K}^p \mathbf{S}^p \mathbf{K}^{p^T}. \tag{8}$$

AMTD
5, 6323–6355, 2012

The second step is the propagation of $\mathbf{S}^e$ into the state vector space which is different to standard error propagation. The inverse model-uncertainty is combined with the Jacobian of the forward operator ($\boldsymbol{K}$):

$$\mathbf{S}^x = (\mathbf{K}^T \mathbf{S}^{e^{-1}} \mathbf{K})^{-1}. \quad (9)$$

Prior- or background knowledge of the retrieval-quantity is not included in this approach.

3.2.2 Information content

An other way of evaluating the retrieval-error is the information content (Shannon and Weaver, 1949) which is an analogy to the concept of entropy in thermodynamics. The information content H provides the "value" of a measurement. It is the reduction in entropy S:

$$H = S(P_1) - S(P_2), \quad (10)$$

where P_1 is the uncertainty before and P_2 after the measurement. For a Gaussian distribution the information content is calculated by:

$$H = 0.5 \log_2(\sigma_a^2) - 0.5 \log_2(\sigma_x^2), \quad (11)$$

where σ_a is the standard deviation due to the natural variability of the parameter and σ_x the uncertainty of the retrieved parameter. H determines the number of possible states of the measurement in binary bits because of the logarithm to the base two. For example: the water vapour column content varies normally between 1 and 70 mm. Can the retrieval derive the water vapour content only with a accuracy of 10 mm H is lower than in case of an uncertainty of 1 mm. After simple logarithm laws the Eq. (11) is basically the quotient of the variances of the retrieval value and its uncertainty and similar to the concept of the signal-to-noise-ratio. Thus, the higher the uncertainty of the retrieval, the lower the information content, the lower the number of possible states that can be resolved based on the measurements.

AMTD
5, 6323–6355, 2012

4 Atmospheric cases and assumptions

In this work, the quantification of uncertainties was performed for a number of different cases. The apparent transmittance of the atmosphere in the near-infrared spectrum is most sensitive to three atmospheric properties: the water vapour column content, the surface albedo and the aerosol optical thickness. Consequently, three cases were considered for each parameter (low, medium and high values) (see Table 1). This results into total number of atmospheric cases of 27. Additionally three other model-parameter-sensitivities were determined: the influence of a cirrus cloud (varying the cirrus optical depth between 0.1 and 1.6), the change of the temperature profile (shifting the temperature profile by a constant offset of ±10 K) and the scale height of an aerosol layer (varying the scale height between 1000 m and 4000 m, homogeneous aerosol layer with 500 m thickness). The theory of optimal estimation requires the knowledge of the uncertainties of the model parameters. The assumed accuracies are given in Table 2 as standard deviations. The influence of other atmospheric properties, such as the Rayleigh optical thickness, carbon dioxide and amounts of other greenhouse gases etc. was assumed to be very low in the wavelength range of interest. Consequently, these parameters were not regarded in this study and kept constant in the simulations.

Since the instruments are not built and calibration errors or signal-to-noise-ratios (SNR) are not determined yet, the measurement errors can only be assumed (guided by the specifications of the concepts). For this reason, a standard SNR of 400 was preconditioned for each channel which is in the approximate range of a NIR-radiance-measurement. The SNR is dependent on the channel width because more energy is coming in with a broader spectral range. However, this quantity turned out to have a non-significant influence and was kept constant. No absolute calibration uncertainty was assumed.

The albedo of natural surfaces is a function of wavelength. In case of real measurements, a common approach to account for this effect is to linearly extrapolate

AMTD
5, 6323–6355, 2012

the surface reflectance in the window channels to estimate the surface reflectance in any spectrally close absorption channel. In the frame of this study, the so-called albedo slope was not considered in the simulations, meaning that for a fixed case the same albedo was used for all simulated channels. However, when calculating the uncertainties, this phenomenon was included with the help of the following. The surface reflectance uncertainty affects the retrieval in two ways:

first, the absolute albedo uncertainty: the uncertainty of the assumed surface reflectance in the window channels, resulting from uncertainties in the atmospheric correction, directly propagates to the uncertainty of the surface reflectance in the absorption channel. However, this error has the same sign in all channels, since the scattering properties do hardly vary within the considered spectral ranges. Since the information used for the water vapour retrieval is provided by the ratio of absorption and window radiances, there is hardly any additional error contribution by the uncertain surface reflectance in the absorption channel. This is reflected by a high correlation of the uncertainties of both reflectance values in the error-covariance-matrix $\mathbf{S}_e$.

Secondly, the albedo slope uncertainty: the correlation of the surface reflectance uncertainties is reduced in cases of a strongly varying albedo slope, resulting in a higher error contribution by the absorption channel. A spectral surface albedo database was analysed with respect to the correlation of the surface reflectance values for different surface types and channel positions. Not surprisingly, the correlation is lower for spectrally distant channels, resulting in less-correlated errors and higher retrieval uncertainties. The error-covariance-matrix $\mathbf{S}_e$ of the model parameters (Eq. 8) was adapted accordingly.

Due to the fact that the spectrometers are not built yet, the instrument-specific response functions are not available yet. Additionally, the shape of response functions has a very low impact on the measured radiance. For convenience, the response function of the MERIS-channel 15 was used. It was adapted to the different scheduled positions and widths (see Figs. 1, 2, 3). In the investigation of the optimal channel distribution this response function was also used.

AMTD
5, 6323–6355, 2012

5 Results

5.1 Uncertainties

Uncertainties in mm of possible water vapour retrievals using the channel distributions of the original concepts of the three planned instruments are shown in Fig. 4. For OLCI and METimage two window channels, close to the $\rho\sigma\tau$-band, were chosen. For MTG only one window and one absorption channel was considered. For the OLCI retrieval two absorption channels and for the METimage retrieval, three absorption channels will be provided. The nominal positions of the considered channels are noted in the legend on the right of Fig. 4. The uncertainties of the 27 cases of a combination of three atmospheric properties are plotted. The legend of these cases is displayed below the plot as coloured bars of total water vapour column (TCWV) in blue, surface albedo (ALB) in yellow and aerosol optical thickness (AOT) in black. Although the uncertainties are discrete points in the reverse logarithmic plot, for better clarity a line was drawn between the points of each albedo class for sun zenith angle 0°. Additionally uncertainties of sun zenith angles of 20° and 60° were calculated and plotted in dashed lines for each instrument.

The most striking feature is that the five-channel combination of the METimage concept (in green) is more certain in almost every case (apart from dark surfaces with low water vapour content) than the others. The four-channel-retrieval of OLCI in red has slightly larger uncertainties than METimage but less than the two-channel retrieval of MTG in purple (apart from cases with a bright surface and medium and high water vapour values). Generally, the uncertainties increase with higher water vapour content. This is due to the fact that absorption lines reach saturation eventually. In other words, the change of the transmittance in a water vapour absorption band approaches zero with higher values (see Fig. 5). Thus, sensitivity of the measurements to TCWV decreases with increasing humidity.

Another finding is the reduction of uncertainties with brighter surfaces, in some cases with one order of magnitude. Brighter surfaces reflect more radiation. Thus, the

AMTD
5, 6323–6355, 2012

measurement is dominated by photons that have not been scattered at atmospheric particles. Above dark surfaces, most of the photons get scattered and thus do not travel through the whole vertical column of water vapour (Lindstrot et al., 2012). Hence, the uncertainty of the aerosol load and scaling height influences primarily the measurement above dark surfaces.

The dependency of the accuracy of the retrievals to the aerosol load is more dissimilar. In case of a bright surface the uncertainty slightly increases with a larger optical thickness of the aerosol layer. In contrast, in case of a dark surface the uncertainty slightly decreases with higher aerosol load. This is due to the fact, that the aerosol layer, located in the lower troposphere, reflects a part of the radiation. Although this radiation does not reach the surface, the presence of the aerosol layer increases the fraction of measured photons that have been scattered in the lower troposphere and thus decreases the error.

To interpret the influence of the errors on the measurement it is more enlightening to examine the uncertainties relatively to the simulated amount of water vapour (not shown here). Generally the relative uncertainties decrease with higher water vapour value. This is consistent because the sensors have limited measurement sensitivities. A very little change in transmittance due to a small water vapour amount can only be determined with low accuracy. In case of MTG, the relative uncertainty exceeds 100 % and in case of METimage and OLCI, it is around 70 % over dark surfaces. The lowest values can be examined over bright surfaces. Again, the higher intensities provide more information for the sensor and thus the uncertainties are smaller. For medium water vapour amounts around 30 mm one has to expect a relative error of around 1 to 10 % depending on the surface and atmospheric circumstances.

To determine the influence of the different viewing geometries and sun zenith angles exemplary uncertainties for two sun zenith angles were calculated and plotted. The impact of sun zenith of 20° on the accuracy is negligible. For dry cases the uncertainties of all retrievals is higher at sun zenith 60° than nadir. This is also true for the MTG

AMTD
5, 6323–6355, 2012

retrieval in the humid cases but not for OLCI and METimage. The uncertainties for OLCI decrease with a higher sun zenith angle.

5.2 Retrievals with one and two absorption channels

In the previous paragraph the behaviour of the scheduled channels was illustrated. The question arises, whether this is the optimal distribution and combination of channels? As seen in Fig. 4 it seems that not only the location but the number of absorption channels has an impact on the accuracy of the retrievals as well. MTG with only one absorption channel has larger uncertainties than the OLCI and METimage with two and three absorption channels.

In the following the METimage channel locations were used exemplary to assume the optimal absorption channel. Figure 6 has the same format as Fig. 4. The five-channel retrieval of METimage is plotted in green again. The other colors account for one-absorption-channel-retrievals with two window channels at 865 and 1020 and one of the three absorption channels, respectively (905 nm in red, 935 nm in purple, 940 nm in dark grey). Obviously the retrievals using only one absorption channel have larger uncertainties than the original METimage setup, in some (dark surface) cases even one order of magnitude. For cases with medium- and high water vapour the lowest uncertainties were found for the retrieval using the absorption channel at 905 nm. The other two have a very low accuracy especially in the humid cases. This is due to the fact that they reach saturation more easily because they are located in a strong absorbing wavelength range. However, this behaviour benefits their accuracy in the dry cases. For low water vapour contents the uncertainties are quite similar. Here the retrievals with channel 19 and 20 are more accurate.

Figure 7 shows the results of the uncertainty calculation of retrievals with two window channels and a combination of two absorption channels (see the legend on the right of the plot). Again the five-channel retrieval is plotted in green. The most evident feature in comparison to Fig. 6 is that the uncertainties are lower in nearly all cases and close to the retrieval using all scheduled channels. The one with the best accuracy is the

AMTD
5, 6323–6355, 2012

combination of channel 18 and 19 because the difference to the five channel retrieval is very low in every case. However, the combination of channel 18 and 20 comes of best in case of bright surfaces. In dry cases the different combinations only differ minimally. In medium and humid cases the combination of 19 and 20 (the strong absorbing channels) is the poorest one. This one also seems to have the strongest sensitivity to the aerosol load.

In summary, retrievals with two absorption channels are more accurate than with one only. The best combination seems to be 905 nm and 935 nm. It is nearly as certain as the original combination of all three absorption channels. The combination of a channel close to the first window channel and one in the strong absorbing range appears to be a good choice.

5.3 Optimal channel setting

In the following, we like to find out whether the channel positions, widths, and their combinations can be improved in order to decrease the uncertainties of a potential water vapour retrieval. For this purpose it is more convenient to examine the information content because it is similar to the relative error and indicates the quality of a measurement on a linear scale. This is shown exemplarily for the METimage buildup.

5.3.1 One-absorption-channel-retrieval

First, the optimal location for a one absorption channel retrieval is wanted. The information content for a retrieval with two window channels (865 and 1020 nm) and one variable absorption channel with a width of 10 nm was calculated. Figure 8 shows the information content as a function of the wavelength (ordinate) and the cases of the atmospheric state which are equivalent to the ones in the last paragraph (abscissa). Each pixel represents the information content of a certain case and a certain center wavelength. Dark pixels account for low and bright for high information contents. Again, in

AMTD
5, 6323–6355, 2012

short, the higher the information content, the higher the number of possible states that can be resolved and the lower the uncertainty of the model.

The most noticeable feature is again the decrement of information content with higher water vapour values. The strong connection between information content and surface albedo is also clear and is represented by the vertical bars of similar brightness. The highest information contents (around 11 bits) were calculated in the dry cases at the strong absorbing channels represented by the bright pixels. Reasons for that were already mentioned in the last chapter. The lowest information contents (represented by dark pixels) were determined in the cases with a high water vapour content and in the strong absorbing wavelength range higher than 925 nm. With changing atmospheric case the information content behaves like described before (apart from 880 and 885 nm), only the magnitudes differ between the channels. If based exclusively on the findings from Fig. 8, it is hard to decide which channel is the best for a water vapour retrieval. On the one hand the maximum information content can be seen at 935 nm and 950 nm, but only for dry cases. On the other hand, these give only little information for humid cases. Hence, it is more convenient to analyse the information content averaged over all cases.

The mean, minimum and maximum information content of all cases as well as the standard deviation is displayed in Fig. 9 as a function of the simulated channels. As before, the strongly absorbing channels show the highest information content but at the same time provide almost no information for humid cases, which is contrary to the desired behaviour of a water vapour retrieval. The goal is to use an absorption channel which is least dependent on the atmospheric case. Looking at the mean which is represented by the dashed line, two maxima appear at 900 and 915 nm which indicate a relatively high information content over all cases.

5.3.2 Two-absorption-channel-retrieval

The information content of a two-absorption-channel-retrieval is displayed in Fig. 10 with a similar logic as in Fig. 8. One absorption channel is at 900 nm (width 10 nm)

AMTD
5, 6323–6355, 2012

and the other one at the location indicated at the ordinate (width again 10 nm). Overall, the information content is increased in comparison to Fig. 8. This is true especially for the strong absorbing range in the humid cases. In this domain the information content increased from nearly zero to 5 bits. The relationship between information content and surface albedo is even more clear here because the sensitivity to the aerosol load is weak. Every albedo class shows almost the same information content. It seems that a spectral channel above 925 nm has to be chosen for the second absorption channel because the information content in this range is high over all cases. A first hint for the best choice is given by the bright pixels at 935 nm.

This can be confirmed with the findings displayed in Fig. 11. The highest mean, maximum and minimum information contents were determined for wavelengths above 925 nm. Outstanding is the maximum at 935 and 950 nm (with a mean of 6.5, respectively 6 bits over all cases). At these wavelengths, the minimum and maximum information content is maximal as well, especially at 935 nm. Thus, a combination of absorption channel at 900 and 935 nm with 10 nm width gives the most information about water vapour.

The water vapour channels of METimage are therefore well designed. The 940 nm channel does not improve the retrieval uncertainties significantly (see Fig. 7). This is probably due to the fact that it is planned to have a width of 50 nm and therefore overlap with the 935 nm and 905 nm (see Fig. 2). Generally, a two absorption channel retrieval is more certain if the absorption channels are least correlated. This was confirmed by cross-correlating all simulated radiances in the different channels (not shown). The lowest correlation coefficient was calculated for the combination of 900 and 935 nm.

6 Summary and conclusion

This study analyses the behaviour and the quantities of the uncertainties of possible water vapour column retrievals using TOA-radiance measurements from future instruments. Depending on the atmospheric state, relative errors of up to 10 % for medium

AMTD
5, 6323–6355, 2012

water vapour values and up to 100 % for very dry cases can be expected. The absolute uncertainties increase with higher water vapour content because of H_2O-saturation. Brighter surfaces reflect more radiation and thus the uncertainty decreases with higher surface albedo. The accuracy decreases slightly with higher optical thickness over medium and bright surfaces. In case of a very dark surface, a thick aerosol layer can increase the accuracy slightly because of the increased amount of radiation which has been reflected in the lower troposphere. The overall uncertainty over all cases turned out to be a function of the number of considered absorption channels. The METimage channel setting with three absorption channels was more accurate than the OLCI setting with two absorption channels and the MTG-FCI with one absorption channel for the most cases. The determination of the optimal position of the absorption channels was done in two steps. First, a retrieval using one absorption channel and the instrument-specific window channels were used to calculate the information content for each atmospheric case. The case-dependent behaviour of the information content is similar to the characteristics of the uncertainties: the information content decreases with higher water vapour values (due to H_2O-saturation), increases with higher surface albedo and decreases slightly with a higher aerosol load. However there are differences in magnitude between the used absorption channels. The optimal position for the "first" absorption channel was determined to be at 900 and 915 nm. The second step was to calculate the accuracy of a retrieval using the window channels, one absorption channel and a second absorption channel with varying position. It turned out, that the second absorption channel is optimal placed in the strong absorbing range above 930 nm. The highest information contents were determined for the combination of 900 or 905 or 915 and 935 nm. This was explained by the low correlation between theses wavelengths. The channel width which has been varied between 10 and 20 nm did not seem to have a strong influence on the information content. A second absorption channel of 20 nm width slightly improved the accuracy of the retrievals (not shown). Consequences for the schedules of the instruments are comparably minor. For the METimage concept the broad 940 nm absorption channel should not be considered. In

AMTD
5, 6323–6355, 2012

the OLCI schedule the location of the second absorption channel should be changed to 935 nm. The 914 nm channel of the MTG-FCI concept seems to be a good choice. Although, for the contentiousness of the time series of water vapour column content, it is recommended to choose the 900 nm channel. Many retrievals and applications already use this setting to determine water vapour. This is why the METimage plan should be changed to an absorption channel combination of 900 and 935 nm.

References

Albert, P., Bennartz, R., and Fischer, J.: Remote sensing of atmospheric water vapor from backscattered sunlight in cloudy atmospheres, J. Atmos. Ocean. Tech., 18, 865, doi:10.1175/1520-0426(2001)018<0865:RSOAWV>2.0.CO;2, 2001. 6325

Albert, P., Bennartz, R., Preusker, R., Leinweber, R., and Fischer, J.: Remote sensing of atmospheric water vapor using the moderate resolution imaging spectroradiometer, J. Atmos. Ocean. Tech., 22, 309, doi:10.1175/JTECH1708.1, 2005. 6325

Bartsch, B., Bakan, S., and Fischer, J.: Passive remote sensing of the atmospheric water vapour content above land surfaces, Adv. Space Res., 18, 25–28, doi:10.1016/0273-1177(95)00285-5, 1996. 6325

Bennartz, R. and Fischer, J.: A modified k-distribution approach applied to narrow band water vapour and oxygen absorption estimates in the near infrared, J. Quant. Spectrosc. Ra., 66, 539–553, doi:10.1016/S0022-4073(99)00184-3, 2000. 6328

Fischer, J. and Grassl, H.: Radiative transfer in an atmosphere-ocean system: an azimuthally dependent matrix-operator approach, Appl. Optics, 23, 1032–1039, doi:10.1364/AO.23.001032, 1984. 6328

Fischer, J. and Leinweber, R. P. R.: Retrieval of total water vapour content from MERIS measurements algorithm theoretical basis document ATBD 2.4, Free University Berlin, Institute for Space Science, Berlin, 2010. 6325

Gao, B.-C., Goetz, A. F. H., Westwater, E. R., Conel, J. E., and Green, R. O.: Possible near-IR channels for remote sensing precipitable water vapor from geostationary satellite platforms, J. Appl. Meteorol., 32, 1791–1801, doi:10.1175/1520-0450(1993)032<1791:PNICFR>2.0.CO;2, 1993. 6325

AMTD
5, 6323–6355, 2012

Grant, I. P. and Hunt, G. E.: Discrete space theory of radiative transfer, I. Fundamentals, P. Roy. Soc. Lond. A Mat., 313, 183–197, 1969a. 6328
Grant, I. P. and Hunt, G. E.: Discrete space theory of radiative transfer, II. Stability and non-negativity, P. Roy. Soc. Lond. A Mat., 313, 199–216, 1969b. 6328
Hollstein, A. and Fischer, J.: Radiative transfer solutions for coupled atmosphere ocean systems using the matrix operator technique, J. Quant. Spectrosc. Ra., 113, 536–548, doi:10.1016/j.jqsrt.2012.01.010, 2012. 6328
Lindstrot, R., Preusker, R., Diedrich, H., Doppler, L., Bennartz, R., and Fischer, J.: 1D-Var retrieval of daytime total columnar water vapour from MERIS measurements, Atmos. Meas. Tech., 5, 631–646, doi:10.5194/amt-5-631-2012, 2012. 6325, 6335
Plass, G. N., Kattawar, G. W., and Catchings, F. E.: Matrix operator theory of radiative transfer, 1: Rayleigh scattering, Appl. Optics, 12, 314–329, doi:10.1364/AO.12.000314, 1973. 6327
Rodgers, C.: Inverse Methods for Atmospheric Sounding: Theory and Practice, World Scientific Pub Co., Oxford, 2000. 6329, 6330
Rothman, L. S., Rinsland, C. P., Goldman, A., Massie, S. T., Edwards, D. P., Flaud, J.-M., Perrin, A., Camy-Peyret, C., Dana, V., Mandin, J.-Y., Schroeder, J., McCann, A., Gamache, R. R., Wattson, R. B., Yoshino, K., Chance, K., Jucks, K., Brown, L. R., Nemtchinov, V., and Varanasi, P.: Reprint of: The HITRAN molecular spectroscopic database and HAWKS (HITRAN Atmospheric Workstation): 1996 edition, J. Quant. Spectrosc. Ra., 111, 1568–1613, doi:10.1016/j.jqsrt.2010.04.019, 2010. 6328
Schluessel, P. and Emery, W. J.: Atmospheric water vapour over oceans from SSM/I measurements, Int. J. Remote Sens., 11, 753–766, doi:10.1080/01431169008955055, 1990. 6325
Shannon, C. E. and Weaver, W.: The Mathematical Theory of Communication, 1949. 6331
Solomon, S.: IPCC (2007): Climate Change, The Physical Science Basis, AGU Fall Meeting Abstracts, pp. D1+, 2007. 6324
Twomey, S., Jacobowitz, H., and Howell, H. B.: Matrix methods for multiple-scattering problems, J. Atmos. Sci., 23, 289–298, 1966. 6328
Wiscombe, W. J.: Improved Mie scattering algorithms, Appl. Optics, 19, 1505–1509, doi:10.1364/AO.19.001505, 1980. 6328

AMTD
5, 6323–6355, 2012

Table 1. Sensitivity simulations input parameter cases.

Property	Low	Medium	High
Water vapour column	1 mm	30 mm	70 mm
Aerosol optical thickness	0.1	0.4	1.0
Surface albedo	0.05	0.2	0.8

AMTD
5, 6323–6355, 2012

Table 2. Sensitivity simulations input parameter uncertainties in unit of standard deviation.

Porperty	Low	Medium	High
Aerosol optical thickness	0.05	0.05	0.05
Surface albedo	0.02	0.03	0.05
Cirrus optical depth	0.1	0.1	0.1
Aerosol scale height	3000 m	3000 m	3000 m
Temperature profile	20 K	20 K	20 K

AMTD
5, 6323–6355, 2012

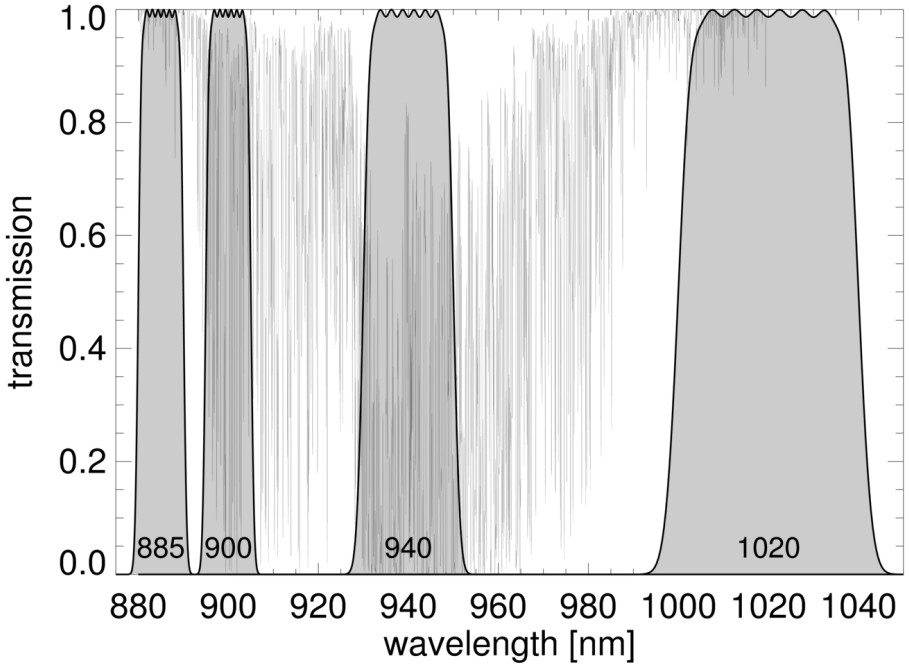

Fig. 1. OLCI channel constellation in the NIR (normalized response functions) and total transmittance of the atmosphere in $\rho\sigma\tau$-band.

AMTD
5, 6323–6355, 2012

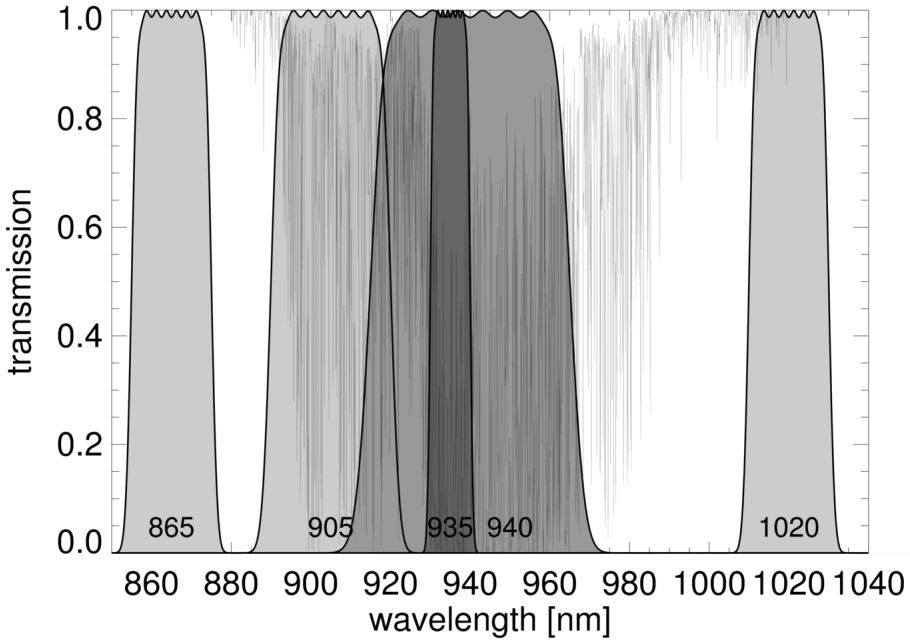

Fig. 2. METimage original channel constellation in the NIR (normalized response functions) and total transmittance of the atmosphere in $\rho\sigma\tau$-band.

AMTD
5, 6323–6355, 2012

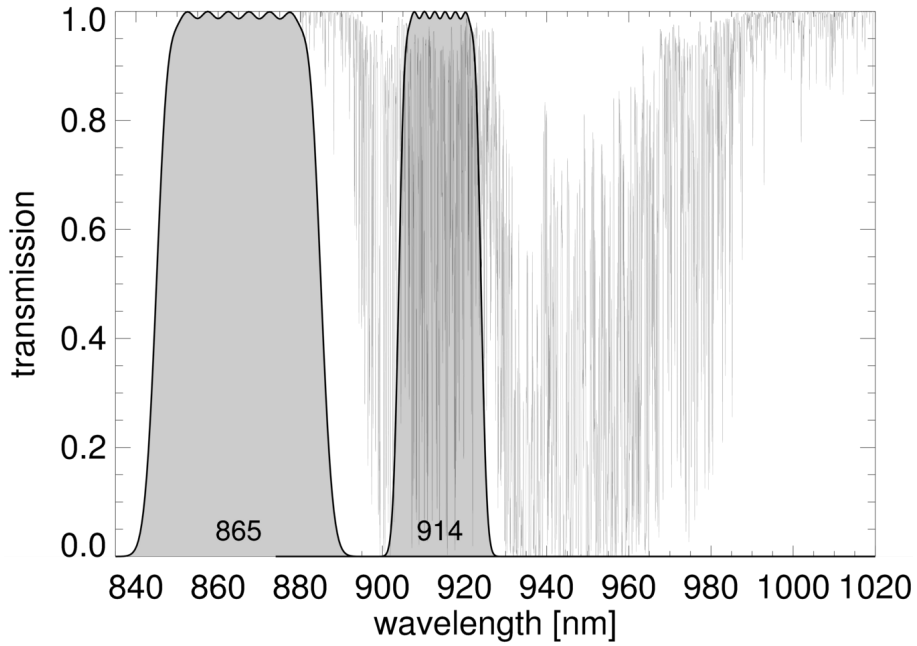

Fig. 3. MTG-FCI original channel constellation in the NIR (normalized response functions) and total transmittance of the atmosphere in $\rho\sigma\tau$-band.

AMTD
5, 6323–6355, 2012

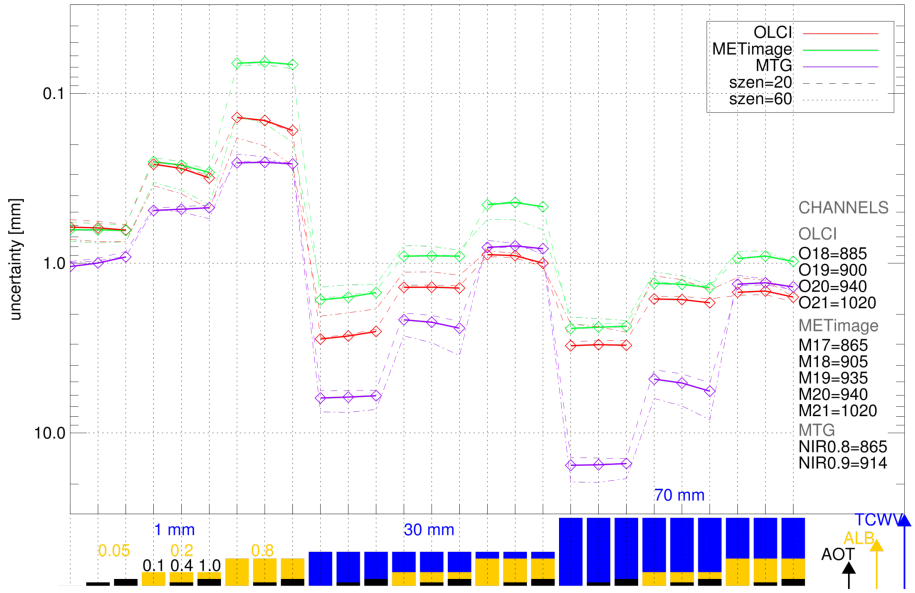

Fig. 4. Uncertainties of water vapour retrievals in mm of three channel combinations of future instruments (OLCI, METimage, MTG) for 27 different cases of a combination of three atmospheric properties: total column water vapour (TCWV), albedo (ALB), and aerosol optical thickness (AOT); for three different zenith angles.

AMTD
5, 6323–6355, 2012

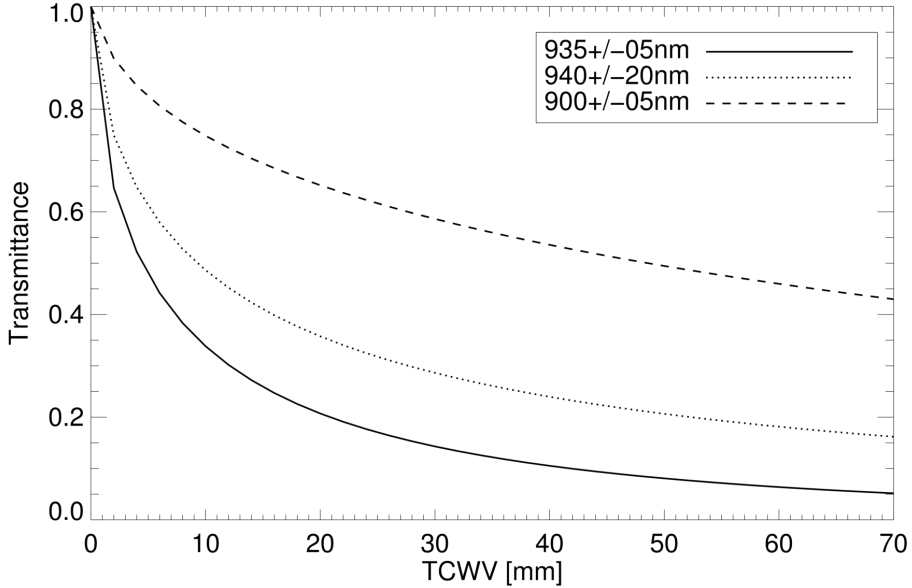

Fig. 5. Transmittance (only absorption) of three different channels in the near infrared with different widths versus TCWV in mm.

AMTD
5, 6323–6355, 2012

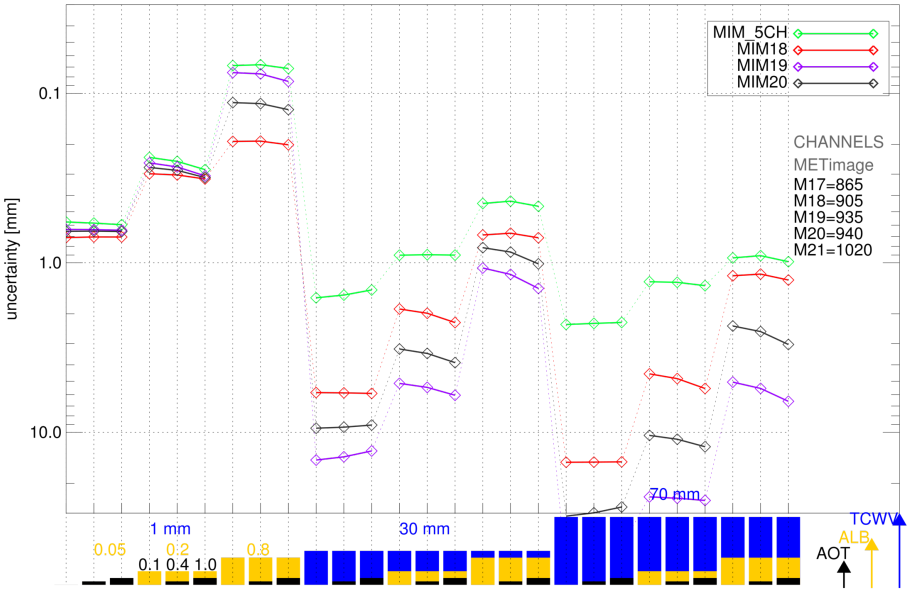

Fig. 6. Uncertainties in mm of water vapour retrievals using one absorption channel and two window channels (METimage concept) for 27 different cases of a combination of three atmospheric properties: total column water vapour (TCWV), albedo (ALB), and aerosol optical thickness (AOT).

AMTD
5, 6323–6355, 2012

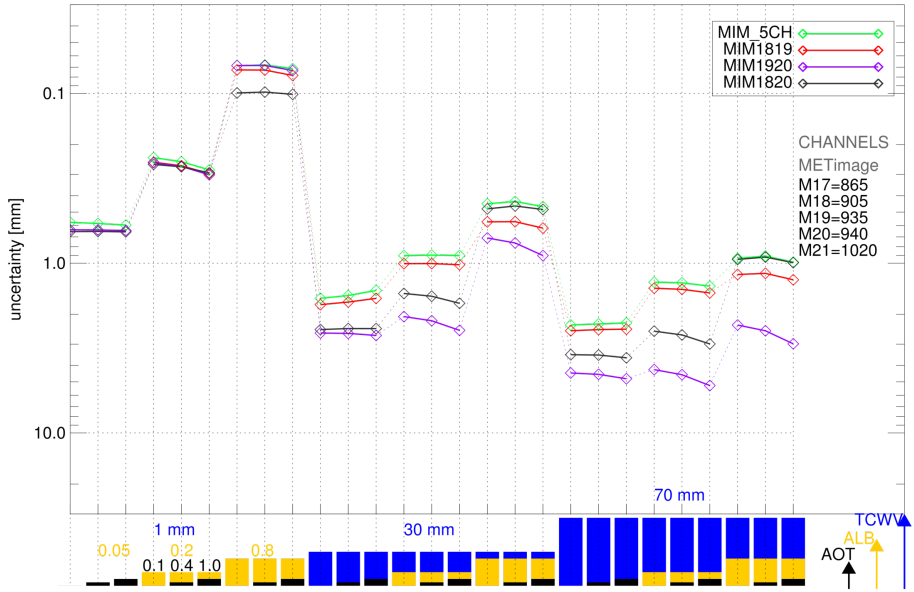

Fig. 7. Uncertainties in mm of water vapour retrievals using two absorption channels and two window channels (METimage concept) for 27 different cases of a combination of three atmospheric properties: total column water vapour (TCWV), albedo (ALB), and aerosol optical thickness (AOT).

AMTD
5, 6323–6355, 2012

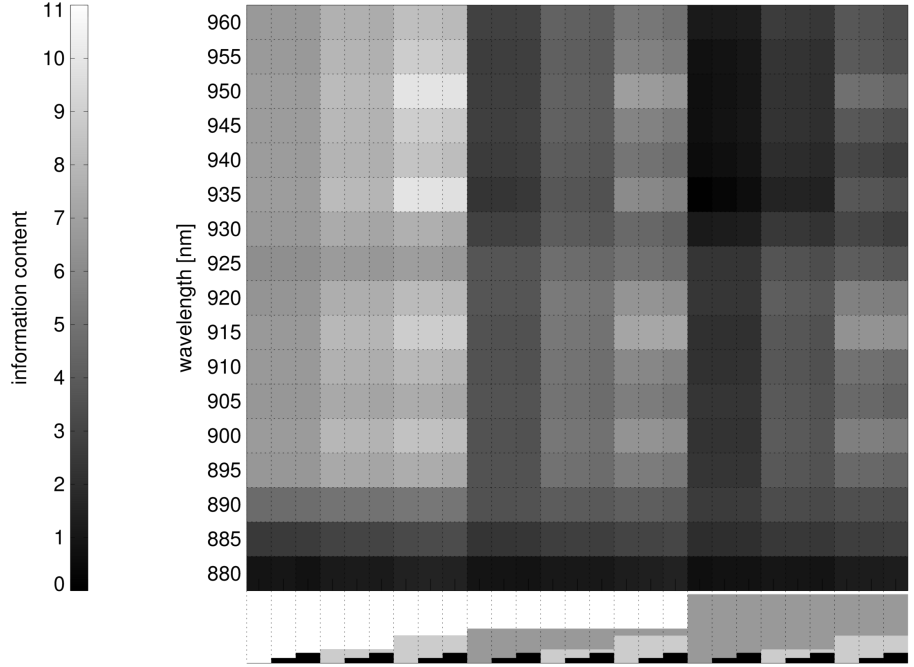

Fig. 8. Information content concerning water vapour of a retrieval using two window channels (METimage: 865, 1020 nm) and one absorption channel (width 10 nm, nadir view) for 27 cases of different atmospheric circumstances (abscissa with legend equivalent to Fig. 4).

AMTD
5, 6323–6355, 2012

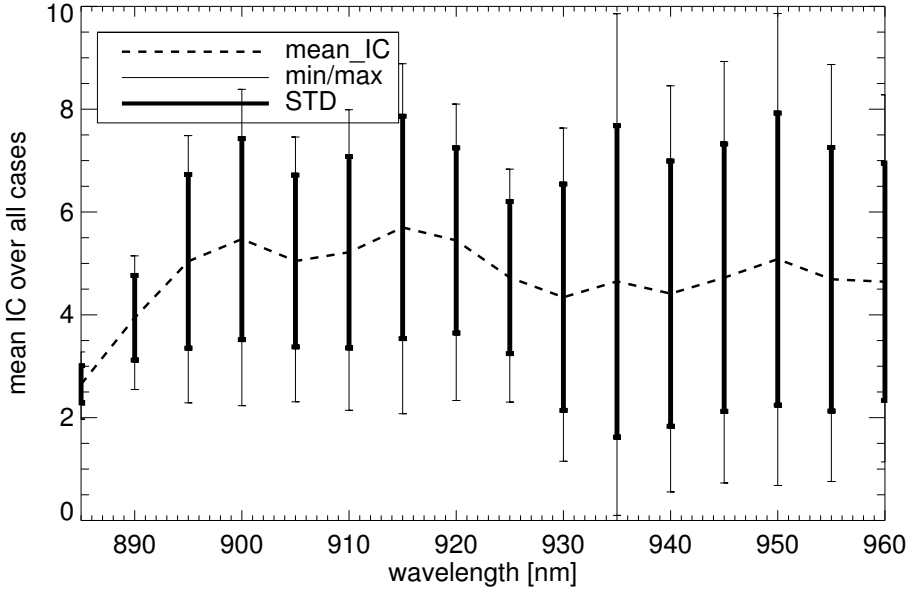

Fig. 9. Mean information content in 27 cases of different atmospheric circumstances concerning water vapour of a retrieval using two window channels (METimage: 865, 1020 nm) and an absorption channel (width 10 nm) (broad bars account for the standard deviation of the cases).

AMTD
5, 6323–6355, 2012

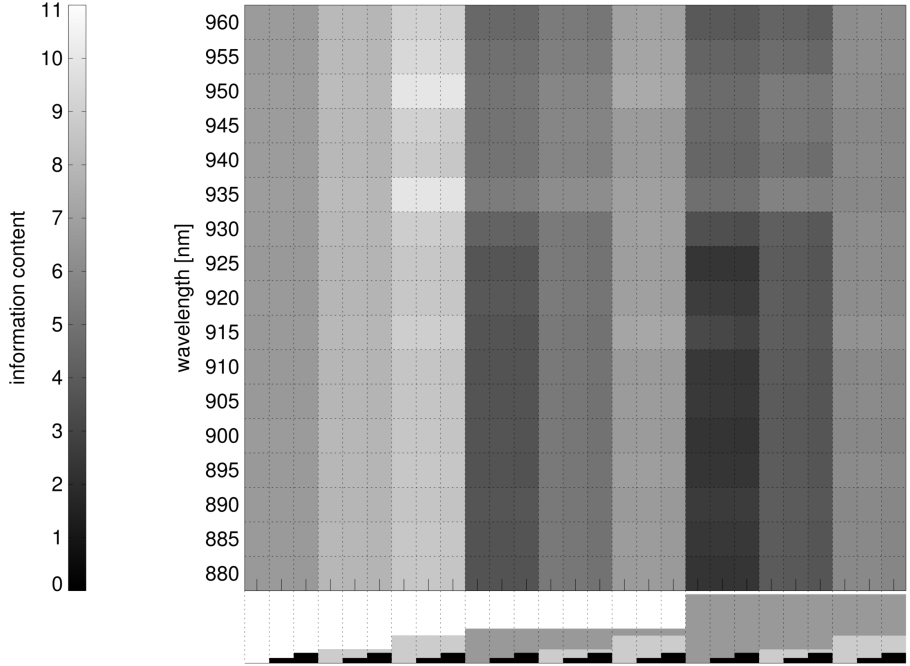

Fig. 10. Information content concerning water vapour of a retrieval using two window channels (865, 1020 nm), 900 nm and a second absorption channel (width 10 nm) for 27 cases of different atmospheric circumstances (nadir view).

AMTD
5, 6323–6355, 2012

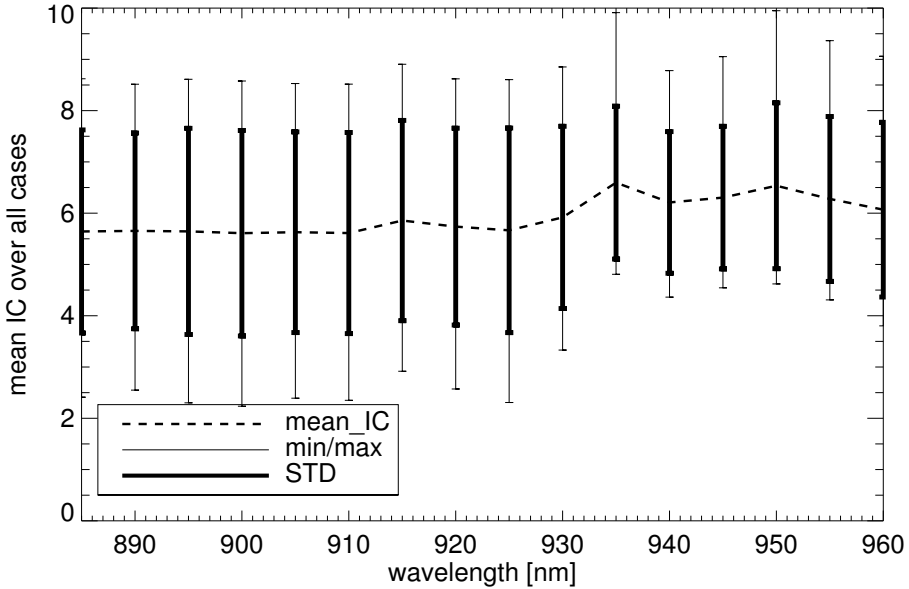

Fig. 11. Mean information content in 27 cases of different atmospheric circumstances concerning water vapour of a retrieval using two window channels (865, 1020 nm), the 900 nm and a second absorption channel (width 10 nm) (broad bars account for the standard deviation of the cases).

AMTD
5, 6323–6355, 2012